Analysis of Chladni Figures

Jacob Buchanan
Adviser: Dr. David Heddle

April 11, 2023

1 Abstract

When a metal plate is vibrated at particular frequencies, interesting patterns can be seen if the plate is covered in a thin layer of sand. This happens because the waves traveling through the plate cancel out at certain points, causing the sand to settle at those points. This phenomenon is attributed to Ernst Chladni, and the patterns are now known as Chladni figures. The study of wave motion in a material is important to the design of structures. The goal of this project is to predict the Chladni figures formed on a square plate at a given frequency. A set of figures will be generated on a square steel plate using a function generator and mechanical wave driver. A theoretical model will be written in Wolfram's Mathematica software to output an image of the figure formed at a given frequency. The computed and observed figures will be compared. The theoretical model requires information about the properties of the plate that are not easily measurable. Rather than attempting to measure these quantities, this information will be fitted by using the experimental figures and theoretical model. This will return a value containing all information about the material properties of the plate that will be used to generate the final comparison.

2 Introduction

In the late 18th century, a German physicist named Ernst Chladni conducted an experiment known to be one of the first attempts at studying the nature of sound. This experiment involved vibrating a solid plate covered with a thin layer of sand and observing the patterns formed. The results of his experiments are referred to as Chladni figures, and have been well-studied since they were first published in 1787 [1]. Showing how solid plates vibrate in a visually interesting way is both insightful and entertaining. The concepts behind these phenomena are also seen in the way drums/cymbals vibrate. Consider the classic example of a glass being shattered at its resonant frequency. A small glass is likely not enough to cause serious problems, but structural engineers should consider the resonant frequencies of their systems to avoid disaster.

The goal of this experiment is to predict the Chladni figures produced on a certain solid surface at certain frequencies, and verify the results by comparing to experimentally-produced figures.

3 Theory

3.1 Mathematical Model

Chladni figures can be modeled by solving the inhomogenous Helmholtz equation in two dimensions,

$$\nabla^2\Psi(x,y) + k^2\Psi(x,y) = -F(x,y), \tag{1}$$

where k is the driving wave number and $F(x,y)$ represents the driving source. For this experiment, the driving source can be modeled as a point with strength F_0 in the center of the plate of length a [2].

$$F(x,y) = F_0\delta(x - a/2)\delta(y - a/2) \tag{2}$$

Other systems may require different representations of the driving source. According to Kirchhoff-Love plate theory, the relationship between driving frequency and driving wave number is

$$f(k) = C \cdot k^2, \tag{3}$$

where C is a constant based on the properties of the plate. The definition of C is

$$C = \frac{1}{2\pi}\sqrt{\frac{Ed^2}{12\rho(1-\nu^2)}}, \tag{4}$$

with E defined as the Young's modulus, d being the thickness of the plate, ρ being the mass density, and ν being the Poisson's ratio. These quantities can be measured and depend on the material of the plate [3].

Figures form on the plate at resonant frequencies. These resonant frequencies will be determined visually by tuning the driving frequency until a clear pattern forms. The theoretical resonant frequencies are the related to the eigenfrequencies of the system, and the figures formed are related to the eigenmodes. These eigenmodes, specific to a square plate with open ends, are given by

$$\Phi_{n_1,n_2}(x,y) = \frac{2}{a}\cos\left(\frac{n_1\pi}{a}x\right)\cos\left(\frac{n_2\pi}{a}y\right), \tag{5}$$

where a is the side length of the square plate and n_1 & n_2 are non-negative integers. The eigenvalues for these modes are

$$k_{n_1,n_2} = \frac{\pi}{a}\sqrt{n_1^2 + n_2^2}. \tag{6}$$

These eigenvalues and eigenmodes are simpler than a normally observed pattern on the plate. This is because the observed figures are a combination of various eigenmodes,

$$\Psi(x,y) = \sum_n A_n\Psi_n(x,y). \tag{7}$$

Using the orthogonality of modes and integrating over the surface, the constant A_n can be found [4].

$$A_n = \frac{\Psi_n(a/2, a/2)}{k_n^2 - k^2} \tag{8}$$

This results in the following equation for the Chladni plate,

$$\Psi(x, y) = \sum_{n_1, n_2} \frac{\Psi_{n_1,n_2}(a/2, a/2)\Psi_{n_1,n_2}(x, y)}{k_{n_1,n_2}^2 - k^2}. \tag{9}$$

Equation (9) where $\Psi(x, y) = 0$ can be plotted to visualize Chladni figures.

3.2 Data Analysis

One metric for comparing experimental and theoretical figures a mean-squared error calculation. The experimental data and theoretical model was compared using a binary image format. The mean squared error is defined as

$$\text{MSE} = \frac{1}{n} \sum_{i=1}^{n} \left(Y_i - \hat{Y}_i \right)^2, \tag{10}$$

where Y_i is the experimental value and $\hat{Y}_i$ is the theoretical value. Because of the information being binary, this value will range between 0 and 1, with 0 being ideal.

Rather than computing C using equation (4), the constant was fit to the data. A nonlinear least squares fitting method was applied to find the constant C in equation (3). A large number of images were generated with a range of k values that covered the frequencies where data was collected. The value for C calculated using equation (4) was used here. A boundary of around 20% of the minimum and maximum was added to ensure the entire range of wave-numbers was accounted for. For every experimental figure photographed, the best fitting value of k was determined by applying the mean-squared error described above. This allows frequency vs. wave-number to be plotted. The nonlinear least squares method was applied to fit the C constant in $f = C \cdot k^2$, with the initial guess being the calculated value.

To measure the success of the theoretical model, the percent error between the k value that best matches the experimental figure and the k value calculated using the fitted C constant was calculated. The percent error is defined as

$$\text{Error} = \frac{|k_{fit} - k_{exp}|}{k_{exp}} \cdot 100. \tag{11}$$

While the mean-squared error is acceptable for comparing the figures in image format, comparing the difference in wave number was found to be more effective.

4 Methods

4.1 Experimental Figures

Creating Chladni figures in the lab was a straightforward task. A function generator and mechanical vibrator were connected to Chladni plate kit (described further in Appendix A) which allowed for easy control of the driving frequency. A small amount of sand-like particles were poured onto the plate. The frequency was set to 100 Hz and increased slowly. The voltage was adjusted as necessary. When a resonant frequency was found, the vibrations in the plate would become noticeably louder even at a constant voltage. A Chladni figure would also form on the plate at these loud frequencies. The volume of the plate at resonant frequencies varied. Some were loud at low voltages and had clear figures, while some required the maximum-allowed power output to appear clearly.

For every Chladni figure formed on the plate that was found, an iPhone camera was used to photograph the plate. The camera had to be leveled to the plate to minimize errors in the data analysis. A tripod was used to hold the camera, with both the plate and camera leveled to the ground. The photo was saved with the frequency in its filename.

Some challenges were encountered throughout this process. Some of the figures were asymmetric, which is not predicted by the theoretical model. This was likely caused by the driving system not being perfectly level and the plate not being perfectly flat. Accounting for this in the theoretical model would be difficult and beyond the scope of this project. To resolve this, a different mechanical vibrator was used. Another challenge is that the lighting of the photo has a notable effect on the data analysis. Glare from overhead lighting on the plate can trick the analysis code into thinking there are particles in places which there are none. This can be improved by tuning the analysis code, but the best solution was to perform the experiment without overhead lighting.

4.2 Theoretical Figures

The figures from the model described in section 3.1 were generated in Wolfram Mathematica. The necessary equations were defined and a contour plot where $\Psi(x, y) = 0$ (see equation (9)) was exported as an image. Mathematica's strength is its ease of use. It also allowed for the computation of multiple plots to be parallelized over all available CPU cores with minimal effort. One challenge faced was the time taken to plot the theoretical Chladni figures. One plot could take around 30 minutes to generate (see appendix A for computer specifications), and hundreds of plots had to be generated in total. This could be resolved by using a more powerful computer at a higher financial cost. The program could also be written in a more efficient language, at the cost of a higher development time.

4.3 Comparison

The data was processed using Python. Every experimental photo was loaded and converted to binary. This required converting to RGB and grayscale, and finally applying a mean threshold. The experimental images were denoised using a Chambolle method in the SciKit-image package. The theoretical images were provided in black and white, but still required

converting to binary using the same methods. Every experimental photo was taken at a resolution of 3024x3024 pixels, so every theoretical image was generated at the same resolution. The two images were converted into a single array using the same method, and these arrays were used to calculate the mean-squared error following equation (10). The choice of experimental vs. theoretical has no effect on the calculation [2].

5 Data

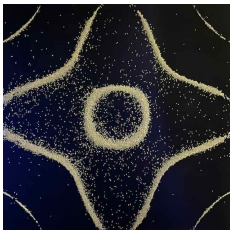	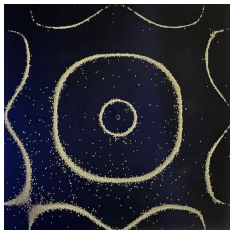	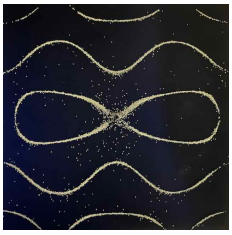	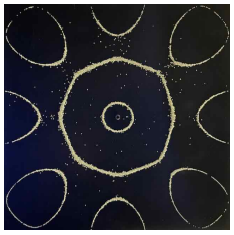	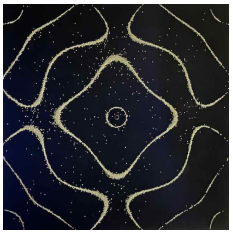
578 Hz	950 Hz	1089 Hz	1223 Hz	1605 Hz
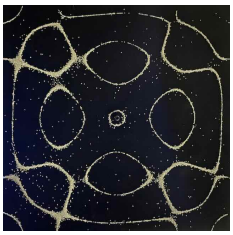	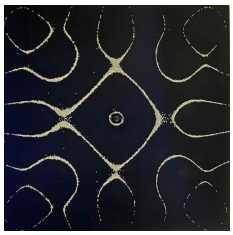	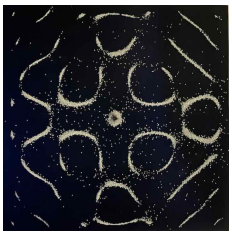	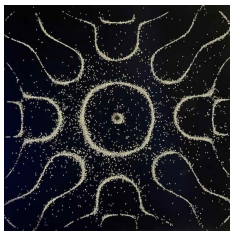	
1939 Hz	2133 Hz	2414 Hz	2595 Hz	3005 Hz
				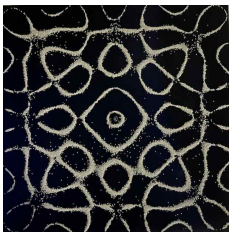
3768 Hz	4130 Hz	4488 Hz	4780 Hz	5338 Hz

Table 1: Experimental figures and frequencies

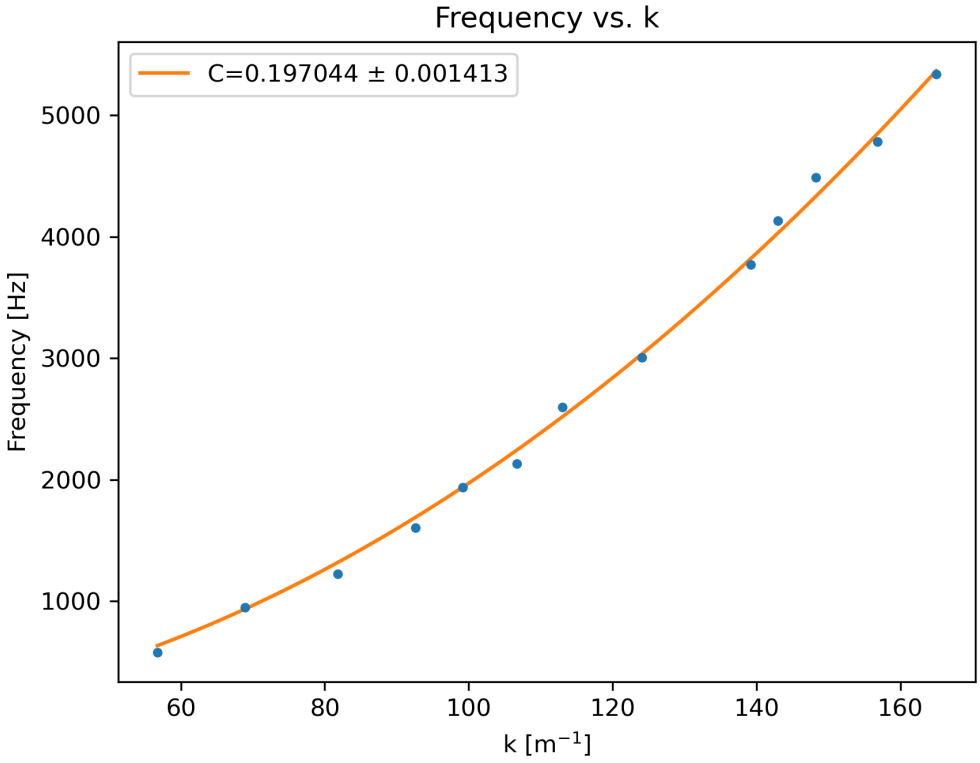

Figure 1: Result of fitting C constant
$C = 0.197044 \pm 0.001413$

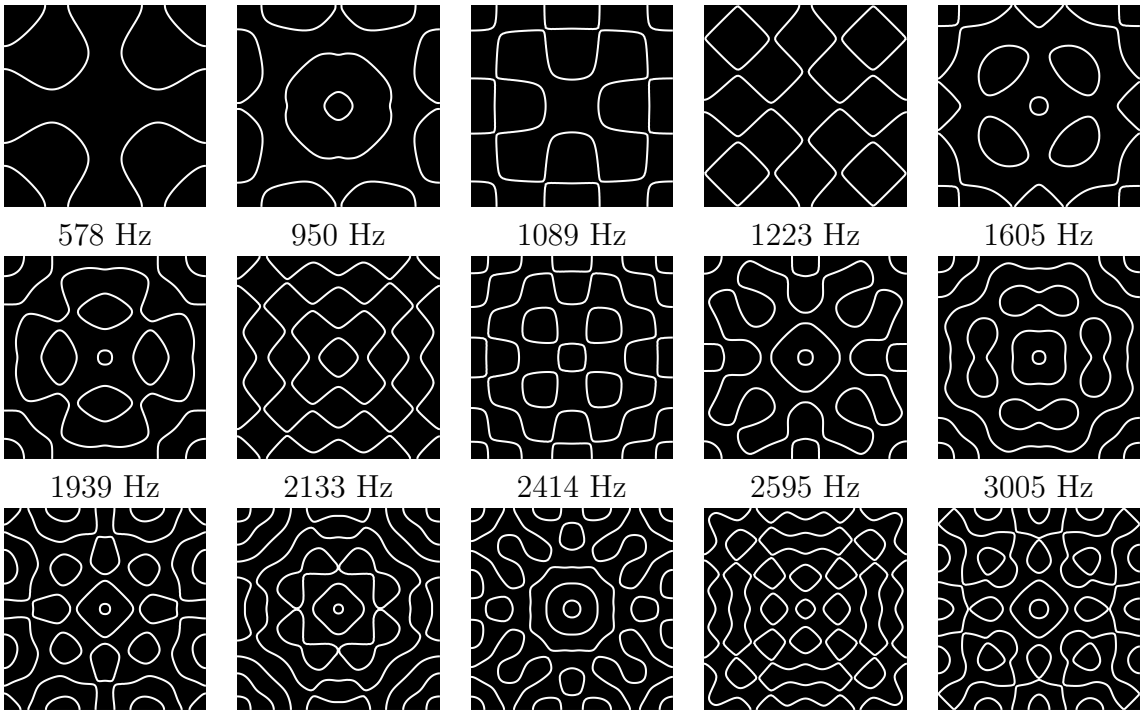

Table 2: Theoretical figures and frequencies using fitted C constant.

Frequency (Hz)	k (m^{-1}) using fitted C	k (m^{-1}) from data	Percent error
578	54.160	56.75	4.563
950	69.435	68.90	0.777
1089	74.342	N/A	N/A
1223	78.783	81.80	3.688
1605	90.252	92.60	2.536
1939	99.199	99.20	0.001
2133	104.043	106.70	2.490
2414	110.685	N/A	N/A
2595	114.759	113.00	1.557
3005	123.493	124.10	0.490
3768	138.285	139.25	0.693
4130	144.775	143.00	1.241
4488	150.919	148.25	1.801
4780	155.752	156.80	0.669
5338	164.592	165.00	0.248

Table 3: Frequency and wave number values with errors. Rows with "N/A" represent frequencies with figures that were not not found in the theoretical model.

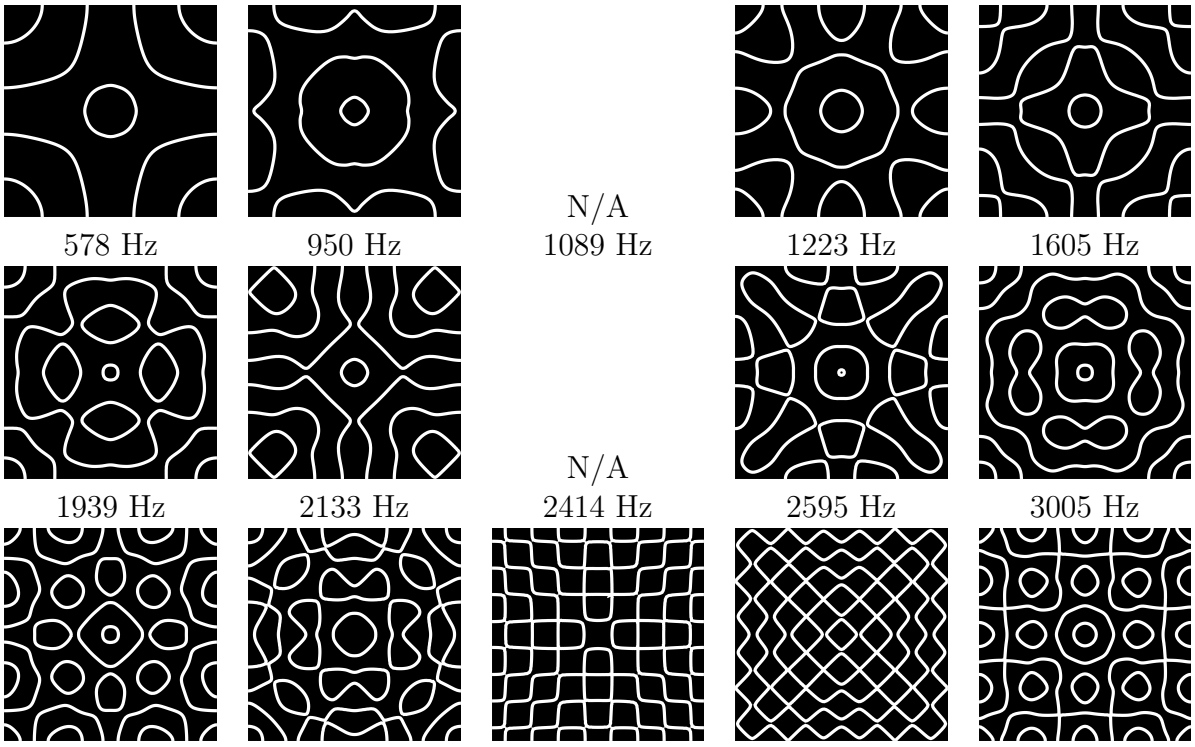

Table 4: Theoretical figures and frequencies that best match Table 1. Values for k used can be seen in Table 3.

6 Discussions and Conclusions

Analyzing the results of this experiment is difficult. The most direct way to study the quality of comparison between experimental and theoretical figures is to look at them side by side. Visually, the theoretical model seems to match the experimental figures fairly well, with some exceptions. For example, the figures at 578 Hz show no obvious agreement between Tables 1 and 2, but the figures at 950 Hz look almost identical. Other figures, particularly at higher frequencies, share many common features. Table 4 shows the figures using wave numbers used to fit the C constant. The figures for 1089 Hz and 2414 Hz were determined to not have matching figures within the model. These look much better as a comparison to the experimental figures, but they do not reflect the entire theoretical model.

While analyzing the figures visually shows the quality of the model, having a numerical comparison is necessary. The percent error between the fitted value for k (Table 2) and the most accurate value (Table 4) is a metric for comparison. The values for the error at each frequency can be found in Table 3. The values overall have low percent errors, with 4.563% being the maximum. While this might imply the experiment is very successful, it does not provide a complete picture of the situation. The range of frequencies where a certain form of figure can be seen on the plate varies. While this was not quantified in this experiment, it has an effect on the results. A higher percent error for one resonant frequency might have figures that seem to compare well because of the wider range of frequencies.

Some experimental figures did not have matching figures in the theoretical model, like

figures at 1089 Hz and 2414 Hz. This is likely caused by the plate not being perfectly flat and the driving system not being perfectly level. They were not used to fit the C constant.

The C constant was found to have a value of $C = 0.197044 \pm 0.001413$. Knowing the plate is made of power-coated mild steel and thickness of 1 ± 0.10 mm, the C constant was calculated to be $C = 0.243344 \pm 0.04$ using equation (4) and values described in Appendix A. The fitted and calculated values of C do not agree within one standard deviation. The values used to calculate the value were not verified, so the lack of agreement is not surprising. The value would also not fit the data.

In conclusion, this model of Chladni figures is not perfect, but overall seems to work well. The standard for a perfect model requires the figures to match for all frequencies, which was not achieved in this experiment. Aside from some anomalies that are likely caused by issues within the experimental setup, the theoretical model did contain the figures that were seen on the plate. One potential improvement to the experiment would be to plot the impedance as a function of frequency. At resonant frequencies, impedance of the system increases. It would be possible to determine the resonance peaks more precisely by looking at a plot of impedance [2]. This would require a more precise function generator to execute well. Including complex damping in the theoretical model would also increase its accuracy, but would add another variable to measure. There are also other potential models other than the inhomogeneous Helmholtz equation that could provide an even more accurate result.

A Equipment Information

1. **PASCO PI-2187 Function Generator**

   This function generator was used to control the mechanical vibrator.

2. **PASCO SF-9324 Mechanical Wave Driver**

   The plate was connected to this mechanical wave driver model.

3. **Mechanical Wave Accessories Bundle from Arbor Scientific**

   This is a kit that contains various wave-related demonstration tools. It requires the function generator and mechanical wave driver to be acquired separately. The square Chladni plate, sand-like particles, and the tool to connect the plate to the wave driver used in this experiment originated from this kit.

   The plate in this kit is composed of powder-coated mild steel. Therefore, the values used in equation (4) were $Y = 200 \pm 10$ GPa [5], $\nu = 0.303 \pm 0.0152$ [6], $\rho = 7850 \pm 392.5$ kg/m^3 [7], and $d = 1 \pm 0.1$ mm. Uncertainties were assumed to be 5% of the value.

4. **Apple MacBook Air M2, 2022 (base model)**

   This laptop was used to generate the theoretical figures and run the analysis code. All time benchmarks are based on this hardware configuration.

References

[1] D. Ullmann, The European Physical Journal Special Topics **145**, 25 (2007).

[2] P. H. Tuan et al., The Journal of the Acoustical Society of America **137**, 2113 (2015).

[3] A. E. H. Love and G. H. Darwin, Philosophical Transactions of the Royal Society of London. (A.) **179**, 491 (1888).

[4] E. J. Skudrzyk, *The Foundations of Acoustics*, Springer Vienna, 1971.

[5] Young's modulus, tensile strength and yield strength values for some materials, 2003, https://www.engineeringtoolbox.com/young-modulus-d_417.html [Accessed April 11, 2023].

[6] Poisson's ratio, 2008, https://www.engineeringtoolbox.com/poissons-ratio-d_1224.html [Accessed April 11, 2023].

[7] Metals and alloys - densities, 2004, https://www.engineeringtoolbox.com/metal-alloys-densities-d_50.html [Accessed April 11, 2023].